CHEMISTRY
A EUROPEAN JOURNAL

FULL PAPER

DOI: 10.1002/chem.201201214

Enantioselective Addition of Cyclic Enol Silyl Ethers to 2-Alkenoyl-Pyridine-*N*-Oxides Catalysed by Cu^{II}–Bis(oxazoline) Complexes

Alessandro Livieri,[a] Massimo Boiocchi,[b] Giovanni Desimoni,[a] and Giuseppe Faita*[a]

Abstract: Asymmetric reactions involving (*E*)-3-aryl-1-(pyridin-2-yl-*N*-oxide)prop-2-en-1-ones and cyclic enol silyl ethers show good yields and excellent enantioselectivities (up to 99.9% *ee*) when catalysed by bis(oxazoline)–Cu^{II} complexes. Different reaction pathways can be followed by different enol silyl ethers: with 2-(trimethylsilyloxy)furan, a Mukaiyama–Michael adduct is obtained, whereas a hetero Diels–Alder cycloadduct was formed by using (1,2-dihydronaphthalen-4-yloxy)trimethylsilane. In the latter reaction, the absolute configuration of the product is consistent with a reagent approach to the less hindered *Re* face of the coordinated substrate in the reactive complex.

Keywords: asymmetric catalysis · copper · cycloaddition · enol silyl ethers · Mukaiyama reactions · nitrogen heterocycles

Introduction

Pyridine-*N*-oxides can act as donor-forming complexes with Lewis acids. If the pyridine ring is functionalised at position 2 with another coordinating group, such as a carbonyl function, this structure can behave as a bidentate ligand. This feature allows the use of 2-carbonyl-pyridine-*N*-oxide derivatives as suitable substrates in metal catalysis. Jørgensen and co-workers[1a] noted that the oxidation of the pyridine nitrogen atom into the corresponding *N*-oxide is indispensable, in order to obtain an appropriate coordination around the Lewis acid. Furthermore, the better coordination ability of the pyridine-*N*-oxides instead the corresponding pyridines in terms of reversible–irreversible coordination to the metal cation has been demonstrated (for example, use of the pyridine-*N*-oxide avoids poisoning of the Osmium-based catalyst in the Sharpless aminohydroxylation).[1b,c] Actually, the first paper about an asymmetric reaction with such derivatives dealt with the asymmetric carbonyl reduction by baker's yeast.[2] If the Lewis acid, usually a metal cation, is coordinated to a chiral ligand (L*), an asymmetric reactive complex is formed. In recent decades, a huge investigation has been made in the field of asymmetric ligands[3] and those with C_2 symmetry emerged as "privileged chiral catalysts".[4] Within C_2-symmetric ligands, bis(oxazoline) (BOX) and, later, pyridine bis(oxazoline) (PyBOX) derivatives gained a preeminent position because of their qualities.[5] Several substrates have been investigated in bis(oxazoline) asymmetric catalysis, and 2-alkenoyl-pyridine-*N*-oxides **1** have emerged as promising substrates in the last five years. This structure provides access to several products due to its wide reactivity (Scheme 1), and it also allows the corresponding reduced pyridine derivatives to be obtained.[6]

The first paper about this topic dealt with the Diels–Alder reaction[7] of **1** acting as a dienophile (Scheme 1a). Later, the enantioselective Friedel–Crafts alkylation with indoles[8a] and pyrroles[8b] catalysed by [Cu^{II}–PyBOX] complexes was investigated (Scheme 1d). Afterwards, the inverse-electron-demand hetero Diels–Alder reaction[9] with electron-rich alkenes was explored, as well as the asymmetric 1,3-dipolar cycloaddition,[10] which was further investigated by Barroso et al. (Scheme 1b,c).[11] More recently, the Michael addition of malonates to 2-alkenoyl-pyridine-*N*-oxides was usefully catalysed by Zn^{II}–BOX complexes (Scheme 1e).[12]

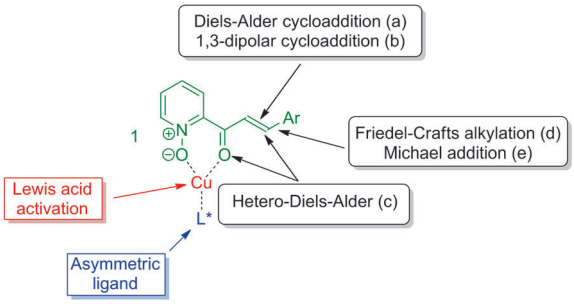

Scheme 1. Structure and reactivity in the asymmetric catalytic processes of 2-alkenoyl-pyridine-*N*-oxides **1**.

[a] Dr. A. Livieri, Prof. G. Desimoni, Prof. G. Faita
Department of Organic Chemistry
University of Pavia
V. le Taramelli, 10; 27100 Pavia (Italy)
Fax: (+39) 0382-987323
E-mail: faita@unipv.it

[b] Dr. M. Boiocchi
Centro Grandi Strumenti
University of Pavia
V. Bassi, 8; 27100 Pavia (Italy)

Supporting information for this article is available on the WWW under http://dx.doi.org/10.1002/chem.201201214.

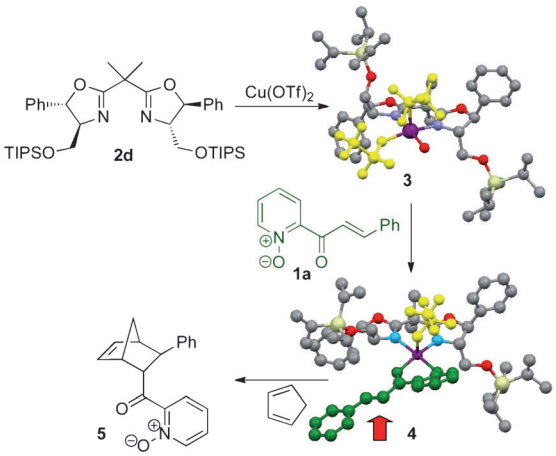

Scheme 2. Structures of the Cu^{II}-based complex with BOX **2d** and the corresponding reactive intermediate with **1a**, which reacts in a Diels–Alder reaction to give the cycloadduct **5**. TIPS: triisopropylsilyl; Tf: trifluoromethanesulfonyl.

In a previous paper, the Cu^{II} complex of a new BOX was isolated and characterised by X-ray diffraction (**3**, Scheme 2).[13] By starting from this complex, the structure of the reactive intermediate involving substrate **1a** was then determined by X-ray crystal analysis of complex **4**.[11] The reacting substrate, **1a**, is coordinated to the cation by its two oxygen atoms to form a square-pyramidal complex, as observed in other structures in which oxygen coordination leads to square-planar geometries; this reflects the larger d-orbital splitting of the cation.[14]

The Diels–Alder cycloaddition of cyclopentadiene to **4** gave cycloadduct **5** with quantitative yields and with almost total control of the stereochemistry, with a stereochemical outcome that was fully consistent with a diene approach to the less hindered *Re* face of the coordinated dienophile.

In this paper, the scope of catalyst **3** to new reactions will be explored. In particular, the addition of different cyclic enol silyl ethers to **1**, to give both cyclic and open chain adducts, will be described.

Results and Discussion

(*E*)-Cinnamoyl-pyridine-*N*-oxides **1** were prepared according to the procedure reported in the literature.[9] This preparation includes the oxidation of 2-acetylpyridine to the corresponding *N*-oxide by *meta*-chloroperoxybenzoic acid (*m*CPBA), followed by condensation under basic conditions with the appropriate aromatic aldehyde to give (*E*)-**1**.

All of the catalysts were $Cu(OTf)_2$ based complexes of the BOX ligands **2a–d** illustrated in Scheme 3. Ligands with structures similar to **2d** have been reported as asymmetric catalysts giving low *ee* values in the epoxidation of carbonyl compounds[15a] and from moderate to high *ee* values in the cyclopropanation of furans.[15b]

The first reaction investigated was the Mukaiyama–Michael addition of 2-(trimethylsilyloxy)furan (**6**) to cinnamo-

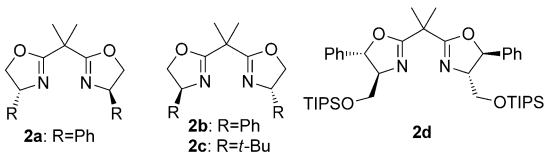

Scheme 3. Structures of the bis(oxazoline) ligands **2a–d** used in this work.

yl-pyridine-*N*-oxide **1a**. The reactions were carried out in anhydrous dichloromethane with 3 Å molecular sieves, and 1,1,1,3,3,3-hexafluoro-2-propanol (HFIP) was used as an additive (Scheme 4). All of the reactions produced discrete (at

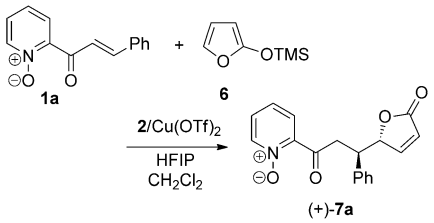

Scheme 4. Mukaiyama–Michael reaction between the (*E*)-cinnamoyl-pyridine-*N*-oxide **1a** and 2-(trimethylsilyloxy)furan (**6**). TMS: trimethylsilyl.

−20 °C) or quantitative yields (at ambient temperature) of the Mukaiyama–Michael products (Table 1). The reaction is highly stereoselective, because only adduct *anti*-**7a**, the relative configuration of which was confirmed by X-ray crystal analysis (Figure 1), was obtained. The absolute configuration of (+)-**7a** cannot be determined from the crystal structure because heavy-element atoms that would cause significant anomalous dispersion effects are not present in the structure and the diffraction data collected with $Mo_{K\alpha}$ radiation are not suitable for absolute structure assignment performed with the probabilistic approach based on Bijovet pair intensity differences.[16]

Table 1. Mukaiyama–Michael reaction between **1a** and **6** in CH_2Cl_2 catalysed by $Cu(OTf)_2$/BOX catalysts (5 mol%).

Entry	Ligand	*T*	*t* [h]	Yield [%]	(+)-**7a** *ee*[a] [%]
1	**2a**	−20 °C	24	75	86
2	**2d**	−20 °C	24	72	80
3	**2a**	RT	18	quant	79
4	**2b**	RT	18	quant	−80[b]

[a] Determined by chiral HPLC (see the Experimental Section). [b] The opposite enantiomer was obtained.

The use of the catalyst based on (*R*)-phenyl-BOX **2a** gave *anti*-**7a** with up to 86% *ee* of the dextrorotatory enantiomer (Table 1, entry 1). An increase in the temperature from −20 °C to ambient temperature allowed a quantitative yield of the adduct to be obtained, although the enantioselectivity decreased (Table 1, entries 1 versus 3). The use of the **2d**-based catalyst, despite the opposite configuration of the C4

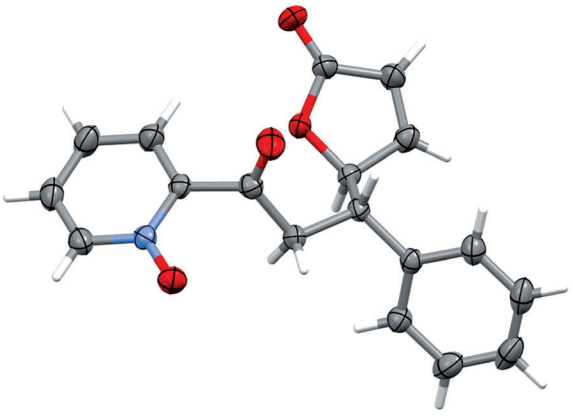

Figure 1. ORTEP view of the X-ray structure of *anti*-**7a** (ellipsoids are drawn at the 30% probability level; red: O, blue: N and grey: C atoms).

stereocentres in the oxazoline rings, produced the same dextrorotatory enantiomer as that obtained by using BOX **2a** (Table 1, entries 1 and 2).

The addition of 1-(trimethylsilyloxy)cyclohexene (**8**) to 2-alkenoyl-pyridine-*N*-oxide **1a** was then investigated (Scheme 5 and Table 2). The reaction proceeded with moderate yields to give a mixture of the diastereomeric products

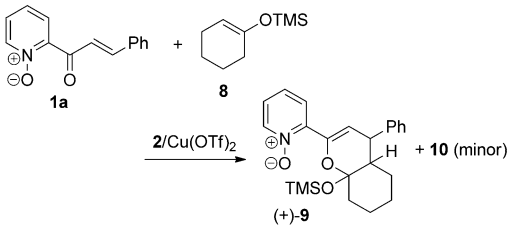

Scheme 5. Reaction between the (*E*)-cinnamoyl-pyridine-*N*-oxide **1a** and 1-(trimethylsilyloxy)cyclohexene (**8**).

Table 2. Reaction between **1a** and **8** in CH_2Cl_2 at −20°C catalysed by $Cu(OTf)_2$/BOX catalysts (5 mol%).

Entry	Ligand	*t* [h]	Equivalents of **8**	Yield [%]	**9**/**10**	(+)-**9** *ee*[a] [%]
1	**2a**	140	1.5	46	85:15	90
2	**2a**	23	3.0	60	95:5	88
3	**2b**	140	1.5	46	86:14	−89[b]
4	**2d**	23	3.0	30	96:4	99

[a] Determined by chiral HPLC (see the Experimental Section). [b] The opposite enantiomer was obtained.

9 and **10**. The two adducts were isolated, but it was not possible to assign the relative configurations of the C4, C4a and C8a stereocentres. However, the relative ratio of the two adducts was determined, and the major one was obtained with diastereomeric ratios ranging from 85:15 to 95:5.

Despite the unknown product structure, it was possible to determine the enantomeric composition of the major adduct (see the Experimental Section for details). The *ee* values were good and the use of the **2d**-based catalyst allowed a single enantiomer to be obtained, even if with moderate reaction yields (Table 2, entry 4). Also in this case, the use of either the **2a**- or **2d**-based catalyst, despite the opposite configurations of the C4 stereocentres of the oxazoline rings, produced the same dextrorotatory enantiomer of **9**.

In order to better understand the reaction mechanism, the study was extended to a benzo-condensed derivative of **8**; the reaction between **1** and **11** was then explored under the same conditions (Scheme 6 and Table 3).

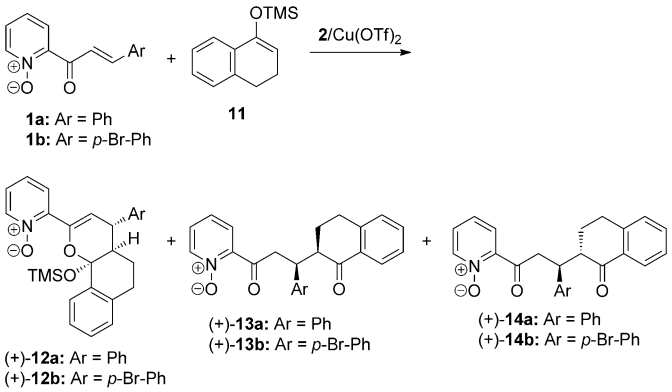

Scheme 6. Reaction between the (*E*)-cinnamoyl-pyridine-*N*-oxides **1a** and **1b** and (1,2-dihydronaphthalen-4-yloxy)trimethylsilane (**11**).

Table 3. Reaction between **1a**,**b** and **11** in CH_2Cl_2 catalysed by $Cu(OTf)_2$/BOX catalysts (5 mol%).

Entry	Ligand	*t* [h]	*T* [°C]	Yield [%]	**12**/**13**/**14**	(+)-**12** *ee*[a] [%]	(+)-**13** *ee*[a] [%]
1	**2a**	70	−20	99	65:29:6	−35[b]	65
2	**2b**	70	−20	99	71:25:4	36	−70[b]
3	**2c**	15	−20	95	49:44:7	99	75
4	**2d**	1	−20	82	71:22:7	99.9	n.d.[c]
5	**2d**	15	−20	94	20:69:11	99.9	99
6	**2d**	140	−70	99	85:13:2	99.9	n.d.[c]
7[d]	**2d**	60	−20	67	20:66:14	99.8	98

[a] Determined by chiral HPLC (see the Experimental Section). [b] The opposite enantiomer was obtained. [c] n.d.: not determined. [d] Reaction carried out with **1b** instead of **1a**.

The reaction proceeded with almost quantitative yields, and three products were isolated from the reaction mixture: the hetero Diels–Alder adducts **12a**,**b** and the *syn*/*anti* products **13a**,**b** and **14a**,**b** (Table 3).

The use of the Ph-BOX-based catalysts did not show a particular selectivity, because the ratio of **12** to **13**+**14** was about 2:1, and all of the products were obtained with low to moderate enantioselectivities (Table 3, entries 1 and 2). The *t*Bu-BOX-based catalyst strongly increased the enantioselectivity of the reaction, and the major reaction product, (+)-**12**, was obtained with up to 99% *ee* (Table 3, entry 3).

The structures of (+)-**12a** and (+)-**13a** were determined by X-ray analysis, allowing (+)-**12a** to be assigned with the (4*S*,4a*R*,10b*R*) absolute configuration (Figure 2). The *cis*

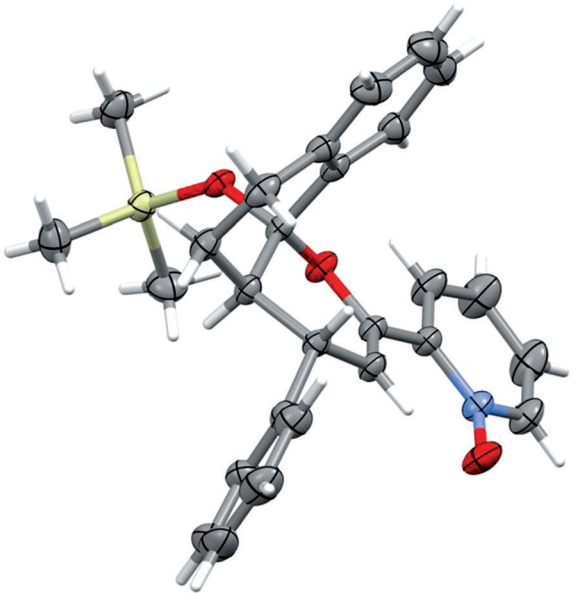

Figure 2. ORTEP view of the X-ray structure of (+)-(4*S*,4a*R*,10b*R*)-**12a** (ellipsoids are drawn at the 30% probability level; red: O, blue: N, grey: C and yellow: Si atoms).

configuration of the 4a and 8a substituents is in agreement with a hetero Diels–Alder mechanism, with dienophile **11** approaching with an *endo* approach to the *Re* face of **1**.

For the open-chain product (+)-**13a**, the absolute configuration cannot be directly assigned because no heavy elements are present; however, the X-ray crystal structure (Figure 3) clearly confirmed the *syn* disposition of the substituents in (+)-**13a**.

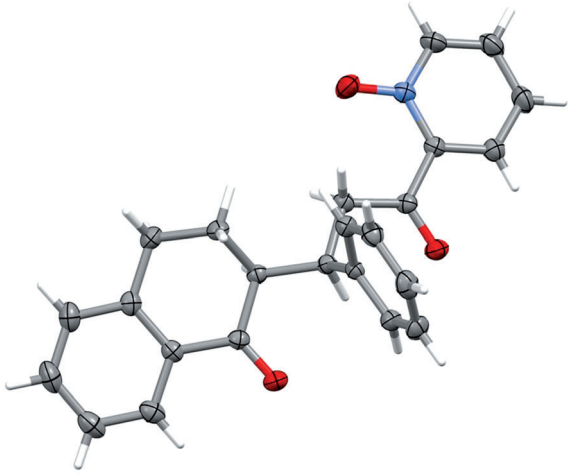

Figure 3. ORTEP view of the X-ray structure of (+)-(*R*,*S*)-**13a** (ellipsoids are drawn at the 30% probability level; red: O, blue: N and grey: C atoms).

More interesting results were obtained with the **2d**-based chiral catalyst. If the reaction was performed for a short reaction time (1 h), the major product obtained was (+)-**12** with excellent enantioselectivity (Table 3, entry 4). The application of prolonged reaction times shifted the reaction selectivity towards the formation of the open chain product (+)-**13a** (Table 3, entry 5), whereas if the reaction was performed at a lower temperature (−70 °C), the favoured reaction product was again the hetero Diels–Alder adduct (+)-**12a** (Table 3, entry 6). A simple explanation of these results may be proposed by considering (+)-**12a** as a primary reaction product that, under prolonged reaction times at higher temperatures, opens into (+)-**13a**. This rationale was easily confirmed by stirring (+)-**12a** at ambient temperature for 8 h in CH_2Cl_2 with a catalytic amount of $Cu(OTf)_2$. The starting product was totally converted into (+)-**13a** with total retention of the enantiomeric purity (99.9% *ee*) (Scheme 7). Consequently, these data allowed us to assign the absolute configuration of structure **13** by considering the retention of configuration at the benzylic stereocentre.

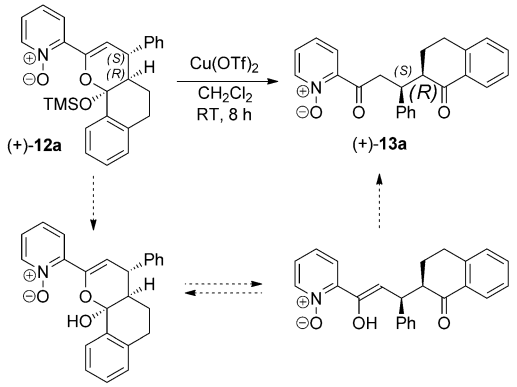

Scheme 7. Proposed mechanism for the conversion of (+)-**12a** into (+)-**13a**.

Product (+)-**14a**,**b** has been also prepared by Michael addition of α-tetralone (**15**) to **1a**,**b** (Scheme 8). This reaction is slower than that reported in Scheme 6, and higher temperature (from −20 °C to room temperature), a nucleophile

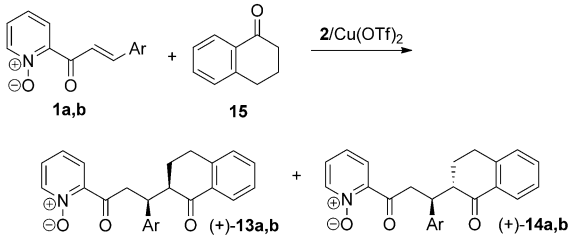

Scheme 8. Reaction between the (*E*)-cinnamoyl-pyridine-*N*-oxides **1a** and **1b** and α-tetralone (**15**).

excess (from 3 to 25 equiv), higher catalyst loading (from 5 to 10% mol), and prolonged reaction times are required to obtain good reaction yields (Table 4). The **2a**,**b**-based chiral catalysts gave unsatisfactory results: reaction yields and stereoselectivities were moderate and the enantioselectivities

Table 4. Reaction between **1a**,**b** and **15** in CH_2Cl_2 at RT catalysed by Cu-$(OTf)_2$/BOX catalysts (10 mol%).

Entry	Substrate	Ligand	*t* [d]	Yield [%]	**13/14**	(+)-**13** *ee*[a] [%]	(+)-**14** *ee*[a] [%]
1	**1a**	**2a**	20	56	73:27	−25[b]	48
2	**1a**	**2b**	20	53	71:29	26	−35[b]
3	**1a**	**2d**	4	99	92:8	94	8
4	**1b**	**2d**	3	99	82:12	92	n.d.[c]

[a] Determined by chiral HPLC (see the Experimental Section). [b] The opposite enantiomer was obtained. [c] n.d.: not determined.

were negligible. By contrast, the **2d**-based catalyst was more efficient and *syn* selective, and (+)-**13** was obtained with up to 94% *ee* (Table 4, entries 3 and 4).

We focused our attention on ligand **2d**, because it has been developed by our group. Our interest further increased from observing that it allows us to obtain from high to almost complete asymmetric induction. Another point of interest is that we had previously characterised the reactive complex between **1**, Cu^{II} and **2d**. In the reaction of **1a** with enol silyl ether **11**, it has been also possible to determine the *Re* face as the reactive one, as previously observed in either the Diels–Alder reaction of **1** with cyclopentadiene or the 1,3-dipolar cycloaddition with diphenylnitrone.[10] In those reactions, opposite stereochemical outcomes were observed with ligands **2b** and **2d** (or **2c**). There are two explanations for this opposite stereochemical induction, one proposed by Evans et al.[17] and the other by Jørgensen and co-workers.[18] Evans et al. suggested a square-planar structure for both reactive complexes; with **2c** (or **2d**), the reagent approaches the substrate from the opposite side to the bulky *tert*-butyl (or TIPS) group, whereas it would approach *syn* to the phenyl ring with **2b** because of the electronic stabilisation of the transition state. Jørgensen and co-workers explained the reverse of induction with flexibility of the reactive complex (between square-planar and tetrahedral geometries) and the ability of the chiral ligand to rock between pseudo-axial and pseudo-equatorial positions.

In this work, we observed this inversion when **1** reacts with **6** and **8**, but not with **11** and **15**. It should be noted these latter reactions are those in which ligand **2a**,**b** showed the worst catalytic activity leading to low *ee* values. Maybe the determination of the reactive complex between **1**, Cu^{II} and **2a**,**b** would lead to important information about this unusual inversion. This goal has not been reached so far because of non-crystalline behaviour of the complex.

At this stage, it is not possible to determine the reactive pathway followed in the first two reactions. ^{1}H NMR spectra together with NOE experiments suggested different structures for the pyran derivatives **9** and **12**. In particular, it is possible that **9** arose from tandem reactions, with an initial Mukaiyama–Michael addition followed by an intramolecular cyclisation. This curious behaviour has been already reported for analogous reactions of **8** with (*E*)-2-oxo-4-aryl-3-butenoates.[19] Hopefully, crystallisation of **9** will allow us to confirm these theoretical considerations.

Conclusion

Copper triflate complexes with chiral bis(oxazolines) ligands **2** show catalytic activity in the reaction between (*E*)-cinnamoyl-pyridine-*N*-oxides **1a**,**b** and different enol silyl ethers. In particular, asymmetric induction by ligand **2d** gives excellent results in almost all of the reactions tested, with *ee* values up to 99.9%.

The reaction mechanisms have not been deeply investigated, although some spectroscopic data suggest different pathways for derivatives **9** and **12**. The structure of (+)-**12a** confirms that the reaction catalysed by **1d** is a hetero Diels–Alder cycloaddition, in which dienophile component **11** approaches substrate **1** from the less hindered *Re* face.

Experimental Section

General: Melting points were determined by the capillary method and are uncorrected. ^{1}H and ^{13}C NMR spectra were recorded at 300 and 75 MHz, respectively, and COSY and NOE experiments were performed in order to confirm product structures. IR spectra were registered on a Perkin–Elmer RX I spectrophotometer. Optical rotations were measured on a Perkin–Elmer 241 polarimeter. Separation and purification of the products was carried out by column chromatography with Merck silica gel 60 (230–400 mesh). The enantiomeric excesses (*ee*) of the products were determined by HPLC with Daicel columns.

Materials: Dichloromethane was the hydrocarbon-stabilised Aldrich ACS grade, distilled from calcium hydride and used immediately. Other solvents were dried according to standard procedures. Copper triflate was the Aldrich ACS reagent. Powdered molecular sieves (3 Å) from Aldrich were heated under vacuum at 300°C for 5 h and kept in sealed vials in a dryer. 2-Alkenoyl-pyridine-*N*-oxides **1a** and **1b** were prepared as reported in the literature.[8,11]

General method for the enol silyl ether addition reaction: In anhydrous glassware, **2** (0.015 mmol), copper triflate (0.005 g, 0.015 mmol) and pyridine-*N*-oxide derivative **1a** or **1b** (0.3 mmol) were added to a test tube. The reactants were dissolved in freshly dried dichloromethane (0.5 mL) and magnetically stirred for 10 min at room temperature. Then, 3 Å molecular sieves (40 mg) and 1,1,1,3,3,3-hexafluoro-2-propanol (31 μL, 0.3 mmol) were added to the reaction mixture at the appropriate reaction temperature. After 15 min, enol silyl ether **6** (66 μL, 0.4 mmol), **8** (174 μL, 0.9 mmol) or **11** (130 μL, 0.6 mmol) was added to the tube. The reaction was monitored by TLC and stopped after completion. The reaction mixture was quenched in water and extracted with dichloromethane (3× 10 mL), and the organic phase was dried over sodium sulphate. Products were isolated by column chromatography.

Mukaiyama–Michael reaction of 1 with 2-(trimethylsilyloxy)furan (6): 2-((*R*)-3-((*R*)-5-Oxo-2,5-dihydrofuran-2-yl)-3-phenylpropanoyl)pyridine-*N*-oxide (**7a**) was obtained by column chromatography (eluent: ethyl acetate) and recrystallised from ethyl acetate/hexane to give a white solid; m.p. 135–137°C; $[\alpha]_D^{25}=42.2$ ($c=0.4$, $CHCl_3$); ^{1}H NMR ($CDCl_3$, 300 MHz): $\delta=8.16$ (d, 1H, $J=6.3$ Hz), 7.49 (dd, 1H, $J=7.8$, 2.2 Hz), 7.33–7.24 (m, 7H), 6.06 (dd, 1H, $J=5.7$, 1.9 Hz), 5.18 (dt, 1H, $J=8.1$, 1.7 Hz), 3.92–3.72 (m, 2H), 3.64 ppm (q, 1H, $J=7.1$); ^{13}C NMR ($CDCl_3$, 75 MHz): $\delta=195.4$, 172.2, 154.9, 146.4, 140.2, 138.4, 128.7, 128.6, 128.1, 127.9, 127.6, 127.3, 127.1, 126.9, 125.5, 122.0, 85.8, 45.1, 45.0 ppm; chiral HPLC analysis on Chiralpak AD column: eluent: isopropanol/hexane 20:80; flow rate: 1.0 mL min^{-1}; t_R: 30.8 ((+)-**7a**), 34.0 min ((−)-**7a**).

Reaction of 1 with 1-(trimethylsilyloxy)cyclohexene (8): 2-(4-Phenyl-8a-(trimethylsilyloxy)-4a,5,6,7,8,8a-hexahydro-4H-chromen-2-yl)pyridine-*N*-oxide (**9**) was obtained by column chromatography (eluent: ethyl acetate/cyclohexane 4:6) as a colourless oil; $[\alpha]_D^{25}=31.4$ ($c=0.8$, $CHCl_3$); ^{1}H NMR ($CDCl_3$, 300 MHz): $\delta=8.30$ (dt, 1H, $J=6.5$, 0.8 Hz), 7.90 (dd,

1H, J=8.2, 2.0 Hz), 7.82 (d, 1H, J=5.2 Hz), 7.25 (m, 7H), 3.67 (dd, 1H, J=8.0, 5.1 Hz), 2.16 (m, 2H), 1.74 (dt, 2H, J=9.9, 3.1 Hz), 1.63 (m, 2H), 1.41 (m, 2H), 1.04 (dq, 1H, J=12.7, 3.4 Hz), 0.06 ppm (s, 9H); ^{13}C NMR ($CDCl_3$, 75 MHz): δ=143.1, 141.0, 139.9, 139.6, 130.5, 126.5, 125.4, 124.5, 123.7, 122.5, 113.1, 99.1, 43.8, 39.9, 37.8, 26.9, 25.6, 22.4, 1.5 ppm; **10** (minor product): ^{1}H NMR ($CDCl_3$, 300 MHz): δ=8.28 (d, 1H, J=6.6 Hz), 7.87 (dd, 1H, J=8.0, 2.1 Hz), 7.69 (d, 1H, J=4.3 Hz), 7.1–7.3 (m, 7H), 3.53 (t, 1H, J=4.5 Hz), 2.14 (m, 2H), 1.8–1.2 (m, 7H), 0.95 (m, 1H), 0.06 ppm (s, 9H); chiral HPLC analysis on Chiralpak AD column: eluent: isopropanol/hexane 10:90; flow rate: 1.0 mL min^{-1}; t_R: 8.9 (**10**), 9.4 ((+)-**9**), 15.3. (**10**), 33.5 min ((−)-**9**).

Reaction of 1a with (1,2-dihydronaphthalen-4-yloxy)trimethylsilane (11): 2-((4*S*,4a*R*,10b*R*)-4-Phenyl-10b-(trimethylsilyloxy)-4a,5,6,10b-tetrahydro-4H-benzo[*h*]chromen-2-yl)pyridine-*N*-oxide ((−)-**12a**) was obtained by column chromatography (eluent: ethyl acetate/cyclohexane 1:1) and recrystallised from ethyl acetate/ligroine as a white solid; m.p. 161–163 °C; $[\alpha]_D^{25}$=−69.7 (c=0.4, $CHCl_3$); ^{1}H NMR ($CDCl_3$, 300 MHz): δ=8.40 (dd, 1H, J=6.5, 0.8 Hz), 8.15(dd, 1H, J=8.2, 2.0 Hz), 7.54 (dd, 1H, J=7.8,0.8 Hz), 7.38 (d, 1H, J=2.6 Hz), 7.05–7.15 (m, 9H), 3.36 (dd, 1H, J=10.7, 2.6 Hz), 3.08 (ddd, 1H, J=18.8, 10.5, 7.5 Hz), 2.93 (dd, 1H, J=18.8, 7.3 Hz), 2.36 (m, 2H), 1.77 (m, 1H), 0.12 ppm (s, 9H); ^{13}C NMR ($CDCl_3$, 75 MHz): δ=142.5, 142.3, 141.1, 139.7, 136.8, 136.2, 128.8, 128.1, 127.8, 126.3, 125.7, 124.7, 124.4, 123.5, 122.8, 114.0, 99.8, 43.8, 40.5, 23.2, 19.2, 1.2 ppm; chiral HPLC analysis on Chiralpak AD column: eluent: isopropanol/hexane 10:90; flow rate: 1.0 mL min^{-1}; t_R: 7.0 ((+)-**12a**), 8.0 min ((−)-**12a**).

2-((*S*)-3-((*R*)-1-Oxo-1,2,3,4-tetrahydronaphthalen-2-yl)-3-phenylpropanoyl)pyridine-*N*-oxide ((+)-**13a**) was obtained by column chromatography (eluent: ethyl acetate/cyclohexane 1:1) and recrystallised from ethyl acetate/ligroine as a white solid; m.p. 147–149 °C; $[\alpha]_D^{25}$=25.3 (c=0.1, $CHCl_3$); ^{1}H NMR ($CDCl_3$, 300 MHz): δ=8.16 (d, 1H, J=6.2 Hz), 8.00 (d, 1H, J=7.8 Hz), 7.47 (t, 1H, J=7.4 Hz), 7.34–7.16 (m, 10H), 4.13 (dt, 1H, J=11.9, 4.7 Hz), 3.82 (d, 2H, J=7.1 Hz), 3.03 (m, 1H), 2.86 (m, 2H), 2.14 (m, 1H), 1.67 ppm (m, 1H); ^{13}C NMR ($CDCl_3$, 75 MHz): δ=198.7, 195.9, 146.6, 143.1, 141.3, 139.7, 132.8, 132.1, 128.1, 127.84, 127.0, 127.0, 126.1, 126.1, 124.9, 51.8, 46.8, 38.7, 27.1, 25.4 ppm; chiral HPLC analysis on Chiralpak AD column: eluent: isopropanol/hexane 10:90; flow rate: 1.0 mL min^{-1}; t_R: 61.8 ((−)-**13a**), 65.8 min ((+)-**13a**).

2-((*S*)-3-((*S*)-1-Oxo-1,2,3,4-tetrahydronaphthalen-2-yl)-3-phenylpropanoyl)pyridine-*N*-oxide ((+)-**14a**) was obtained by column chromatography (eluent: ethyl acetate/cyclohexane 1:1); $[\alpha]_D^{25}$=14.4 (c=0.1, CH_3OH); ^{1}H NMR ($CDCl_3$, 300 MHz): δ=8.17 (dd, 1H, J=6.5, 0.5 Hz), 8.03 (dd, 1H, J=7.0, 0.5 Hz), 7.45 (dt, 1H, J=7.0, 0.5 Hz), 7.32–7.19 (m, 10H), 4.32 (dt, 1H, J=8.5, 4.2 Hz), 4.10 (dd, 1H, J=17.4, 10.6 Hz), 3.48 (dd, 1H, J=17.4, 4.3 Hz), 2.99 (m, 2H), 2.81 (m, 1H), 2.13 ppm (m, 2H); ^{13}C NMR ($CDCl_3$, 75 MHz): δ=197.8, 195.9, 143.3, 142.0, 139.8, 132.8, 128.1, 127.8, 127.7, 127.0, 126.3, 126.1, 125.9, 124.9, 53.2, 42.6, 39.2, 28.5, 24.2 ppm; chiral HPLC analysis on Chiralpak AD column: eluent: isopropanol/hexane 10:90; flow rate: 1.0 mL min^{-1}; t_R: 71.4 ((+)-**14a**), 74.3 min ((−)-**14a**).

Reaction of 1b with (1,2-dihydronaphthalen-4-yloxy)trimethylsilane (11): 2-((4*S*,4a*R*,10b*R*)-4-(4-Bromophenyl)-10b-(trimethylsilyloxy)-4a,5,6,10b-tetrahydro-4H-benzo[*h*]chromen-2-yl)-pyridine-*N*-oxide ((−)-**12b**) was obtained by column chromatography (eluent: ethyl acetate/cyclohexane 1:1); ^{1}H NMR ($CDCl_3$, 300 MHz): δ=8.24 (dd, 1H, J=6.5, 0.8 Hz), 8.14 (dd, 1H, J=8.2, 2.0 Hz), 7.52 (d, 1H, J=7.8 Hz), 7.47–7.36 (m, 4H), 7.28 (dt, 1H, J=7.7, 1.4 Hz), 7.21–7.14 (m, 5H), 3.31 (dd, 1H, J=10.9, 2.6 Hz), 3.1–2.8 (m, 2H), 2.33 (m, 2H), 1.70 (m, 1H), 0.10 ppm (s, 9H); ^{13}C NMR ($CDCl_3$, 75 MHz): δ=144.4, 143.9, 143.3, 142.2, 138.8, 138.3, 133.4, 131.7, 131.0, 130.41, 128.0, 126.8, 126.6, 125.7, 125.1, 122.2, 115.3, 101.9, 46.0, 42.2, 25.3, 21.3, 3.4 ppm; chiral HPLC analysis on Chiralpak AD column: isopropanol/hexane 10:90; flow rate: 1.0 mL min^{-1}; t_R: 8.2 ((+)-**12b**), 9.5 min ((−)-**12b**).

2-((*S*)-3-(4-Bromophenyl)-3-((*R*)-1-oxo-1,2,3,4-tetrahydronaphthalen-2-yl)-propanoyl)pyridine-*N*-oxide ((+)-**13b**) was obtained by column chromatography (eluent: ethyl acetate/cyclohexane 1:1); $[\alpha]_D^{25}$=35.5 (c=0.8, $CHCl_3$); ^{1}H NMR ($CDCl_3$, 300 MHz): δ=8.16 (d, 1H, J=6.0 Hz), 7.98 (d, 1H, J=7.8 Hz), 7.45–7.19 (m, 10H), 4.16 (dt, 1H, J=14.3, 7.0 Hz), 3.82 (dd, 2H, J=7.5, 2.7 Hz), 3.06–2.79 (m, 3H), 2.12 (m, 1H), 1.66 ppm (m, 1H); ^{13}C NMR ($CDCl_3$, 75 MHz): δ=198.1, 195.4, 146.3, 143.0, 140.3, 139.9, 132.8, 132.0, 130.8, 128.1, 127.2, 127.0, 126.3, 126.1, 125.0, 120.0, 51.6, 46.5, 38.0, 27.4, 25.2 ppm; chiral HPLC analysis on Chiralpak AD column: isopropanol/hexane 20:80; flow rate: 1.0 mL min^{-1}; t_R: 30.9 ((−)-**13b**), 34.6 min ((+)-**13b**).

2-((*S*)-3-(4-Bromophenyl)-3-((*S*)-1-oxo-1,2,3,4-tetrahydronaphthalen-2-yl)-propanoyl)pyridine-*N*-oxide ((+)-**14b**) was obtained by column chromatography (eluent: ethyl acetate/cyclohexane 1:1); ^{1}H NMR ($CDCl_3$, 300 MHz): δ=8.17 (d, 1H, J=6.5 Hz), 8.02 (d, 1H, J=7.0 Hz), 7.47–7.19 (m, 10H), 4.27 (dt, 1H, J=10.6, 4.0 Hz), 4.13 (m, 1H), 3.48 (dd, 1H, J=17.6, 3.9 Hz), 2.98 (m, 2H), 2.81 (dt, 1H, J=12.1, 4.6 Hz), 2.15 ppm (m, 2H); ^{13}C NMR ($CDCl_3$, 75 MHz): δ=197.6, 195.5, 146.1, 143.2, 141.1, 139.9, 132.9, 132.2, 130.9, 129.5, 128.1, 127.2, 127.0, 126.4, 126.2, 125.0, 119.8, 53.0, 42.7, 38.7, 28.5, 24.3 ppm; chiral HPLC analysis on Chiralpak AD column: isopropanol/hexane 20:80; flow rate: 1.0 mL min^{-1}; t_R: 38.7 ((+)-**14b**), 40.6 min ((−)-**14b**).

General method for α-tetralone (15) addition to 1a,b: In anhydrous glassware, **2** (0.03 mmol), copper triflate (0.010 g, 0.03 mmol) and pyridine-*N*-oxide derivatives **1a**,**b** (0.3 mmol) were added to a test tube. The reactants were dissolved in freshly dried dichloromethane (0.5 mL) and magnetically stirred at room temperature. After 15 min, α-tetralone (**15**; 650 μL, 5 mmol) was added to the tube. The reaction was monitored by TLC and stopped after completion. The reaction mixture was quenched in water and extracted with dichloromethane (3×10 mL), and the organic phase was dried over sodium sulphate. The products were isolated by column chromatography with ethyl acetate/cyclohexane (3:7) as the eluent. The ^{1}H and ^{13}C NMR spectra were identical to those found for the products from the corresponding reaction with the enol silyl ether.

X-ray diffraction studies of 7a, 12a and 13a: All crystal structures were solved by direct methods (SIR97)[20] and refined with full-matrix least-

Table 5. Crystallographic data for **7a**, **12a** and **13a**.

	7a	**12a**	**13a**
formula	$C_{18}H_{15}NO_4$	$C_{27}H_{29}NO_3Si$	$C_{24}H_{21}NO_3$
M_r	309.31	443.60	371.42
crystal system	orthorhombic	monoclinic	orthorhombic
space group	$P2_12_12_1$ (no. 19)	$P2_1$ (no. 4)	$P2_12_12_1$ (no. 19)
a [Å]	8.368(2)	9.752(2)	6.094(1)
b [Å]	17.598(3)	11.937(2)	15.840(2)
c [Å]	10.262(3)	10.409(1)	19.215(4)
α [°]	90	90	90
β [°]	90	100.91(1)	90
γ [°]	90	90	90
V [Å^3]	1511.2(6)	1189.8(3)	1854.7(6)
Z	4	2	4
ρ_{calcd} [g cm^{-3}]	1.360	1.238	1.330
μ ($Mo_{K\alpha}$) [mm^{-1}]	0.097	0.127	0.088
$2\theta_{max}$ [°]	25	30	30
min/max transmission	0.959/0.990	0.948/0.990	0.986/1.000
collected reflns	3601	8113	7144
independent reflns	2671	6927	3077
R_{int}	0.023	0.011	0.026
strong refln [$F_o > 2\sigma(F_o)$]	1925	5010	2233
refined parameters	208	292	253
$R1$/$wR2$ (strong data)	0.0422/0.0928	0.0446/0.0926	0.0444/0.0942
$R1$/$wR2$ (all data)	0.0741/0.1082	0.0736/0.1045	0.0693/0.1040
goodness of fit	0.962	1.019	1.017
max/min residuals [e Å^{-3}]	0.16/−0.16	0.21/−0.14	0.16/−0.20
Flack's parameter	n.d.[a]	−0.05(11)	n.d.[a]

[a] n.d.: not determined.

square procedures on F^2 (SHELXL-97)[21] by using all reflections collected on an Enraf–Nonius CAD4 diffractometer ($\lambda = 0.71073$ Å, $T = 293$ K). Lorentz, polarisation and absorption effect (psi-scan method)[22] corrections were applied. H atoms were placed at the calculated positions. Only for **12a**, the absolute configuration was established by anomalous dispersion effects in the diffraction data. Crystal data are reported in Table 5. CCDC 857146 (**7a**), 857147 (**12a**) and 857148 (**13a**) contain the supplementary crystallographic data for this paper. These data can be obtained free of charge from the Cambridge Crystallographic Data Centre via www.ccdc.cam.ac.uk/data_request/cif.

Acknowledgements

This work was supported by the Ministero dell'Università e della Ricerca (MiUR) (PRIN 2008) and by the University of Pavia.

[1] a) A. Landa, A. Minkkilä, G. Blay, K. A. Jørgensen, *Chem. Eur. J.* **2006**, *12*, 3472–3483; b) G. Heimgärtner, D. Raatz, O. Reiser, *Tetrahedron* **2005**, *61*, 643–655; c) D. Raatz, C. Innertsberger, O. Reiser, *Synlett* **1999**, 1907–1910.
[2] M. Takeshita, S. Yoshida, *Heterocycles* **1990**, *30*, 871–874.
[3] R. Noyori, *Asymmetric Catalysis in Organic Synthesis*, Wiley, New York, **1994**.
[4] T. P. Yoon, E. N. Jacobsen, *Science* **2003**, *299*, 1691–1693.
[5] a) G. Desimoni, G. Faita, K. A. Jørgensen, *Chem. Rev.* **2006**, *106*, 3561–3651; b) G. Desimoni, G. Faita, K. A. Jørgensen, *Chem. Rev.* **2011**, *111*, PR284–PR437; c) G. Desimoni, G. Faita, P. Quadrelli, *Chem. Rev.* **2003**, *103*, 3119–3154.
[6] S. Youssif, *ARKIVOC* **2001**, 242–268.
[7] S. Barroso, G. Blay, J. R. Pedro, *Org. Lett.* **2007**, *9*, 1983–1986.
[8] a) P. K. Singh, V. K. Singh, *Org. Lett.* **2008**, *10*, 4121–4124; b) P. K. Singh, V. K. Singh, *Org. Lett.* **2010**, *12*, 80–83.
[9] S. Barroso, G. Blay, M. C. Munoz, J. R. Pedro, *Adv. Synth. Catal.* **2009**, *351*, 107–111.
[10] A. Livieri, M. Boiocchi, G. Desimoni, G. Faita, *Chem. Eur. J.* **2009**, *15*, 516–520.
[11] S. Barroso, G. Blay, M. C. Munoz, J. R. Pedro, *Org. Lett.* **2011**, *13*, 402–405.
[12] S. K. Ray, P. K. Singh, V. K. Singh, *Org. Lett.* **2011**, *13*, 5812–5815.
[13] G. Desimoni, G. Faita, M. Toscanini, M. Boiocchi, *Chem. Eur. J.* **2009**, *15*, 9674–9677.
[14] R. Rasappan, D. Laventine, O. Reiser, *Coord. Chem. Rev.* **2008**, *252*, 702–714.
[15] a) V. K. Aggarwal, L. Bell, M. P. Coogan, P. Jubault, *J. Chem. Soc. Perkin Trans. 1* **1998**, 2037–2042; b) M. Schinnerl, C. Böhm, M. Seitz, O. Reiser, *Tetrahedron: Asymmetry* **2003**, *14*, 765–771.
[16] a) R. W. W. Hooft, L. H. Straver, A. L. Spek, *J. Appl. Crystallogr.* **2008**, *41*, 96–103; b) R. W. W. Hooft, L. H. Straver, A. L. Spek, *J. Appl. Crystallogr.* **2010**, *43*, 665–668.
[17] D. A. Evans, J. S. Johnson, E. J. Oliava, *J. Am. Chem. Soc.* **2000**, *122*, 1635–1649.
[18] J. Thorhauge, M. Roberson, R. G. Hazell, K. A. Jørgensen, *Chem. Eur. J.* **2002**, *8*, 1888–1898.
[19] A. Martel, S. Leconte, G. Dujardin, E. Brown, V. Maisonneuve, R. Rectoux, *Eur. J. Org. Chem.* **2002**, 514–525.
[20] A. Altomare, M. C. Burla, M. Camalli, G. L. Cascarano, C. Giacovazzo, A. Guagliardi, A. G. G. Moliterni, G. Polidori, R. Spagna, *J. Appl. Crystallogr.* **1999**, *32*, 115–119.
[21] G. M. Sheldrick, *Acta Crystallogr. Sect. A* **2008**, *64*, 112–122.
[22] A. C. T. North, D. C. Phillips, F. S. Mathews, *Acta Crystallogr. Sect. A* **1968**, *24*, 351–359.

Received: April 10, 2012
Published online: ■■ ▮▮, 0000

Asymmetric Catalysis

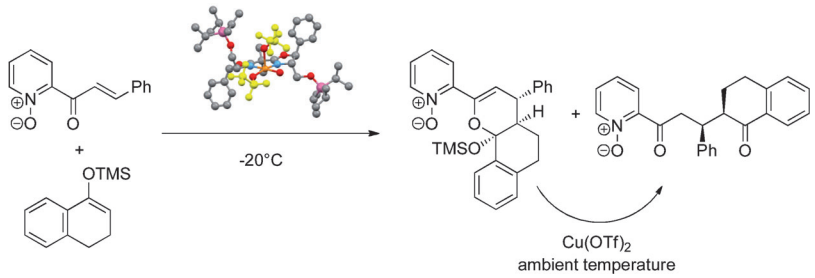

Out of the BOX: Asymmetric reactions involving (*E*)-3-aryl-1-(pyridin-2-yl-*N*-oxide)prop-2-en-1-ones and cyclic enol silyl ethers show good yields and excellent enantioselectivities (up to 99.9% *ee*) when catalysed by Cu^{II}–bis(oxazoline) (BOX) complexes (see scheme; TMS: trimethylsilyl). Mukaiyama–Michael and hetero Diels–Alder pathways can be followed with the different enol silyl ethers.